



ADSORPTION OF METHYLENE BLUE FROM WATER USING GOPANINANOCOMPOSITE

A. N. Ingole^a, S. B. Kapoor^b, D. B. Patil^c

^aDepartment of Chemistry, Government Institute of Science, Nagpur - 440001 (M.S.), India

^b Department of Chemistry, Arts, Commerce & Science College Tukum, Chandrapur-442401, (M.S.), India

^cDepartment of Chemistry, Govt. Institute of Science, Nagpur - 440001 (MS) India
Email: kapoor.sushil2012@gmail.com

ABSTRACT

Methylene blue (MB) being disposed off as a waste in to water resources even in small quantity, poses certain hazards and environmental problems. The objective of this study is to investigate the adsorption of MB from aqueous solution onto hydrothermally synthesized graphene oxide polyaniline (GOPAni) composites. GOPAni composites are firstly characterized using, FTIR, XRD, AND SEM techniques. Batch adsorption experiments were conducted by using the UV-visible spectroscopy and by varying parameters namely: contact time, pH, initial dye concentration and adsorbent dose. The percentage of color removal decreased with increase of initial dye concentration. It was found that the percentage of dye removal was 97% for the GOPAni composite. The Freundlich and Langmuir models were applied to describe the equilibrium isotherms. Equilibrium data were fit to Langmuir isotherm. The Langmuir isotherm fits the MB adsorption data on GOPAni composite. Results obtained indicate that GOPAni composite could be employed as an efficient adsorbent similar to other conventional adsorbents for MB uptake.

Keywords: Adsorption, Methylene blue, GOPAni composites, X-ray diffraction Cationic dye

1. Introduction

Water pollution poses severe damages to the environment, thereby attracting much scientific attention to the removal of various pollutants from aqueous bodies [1]. The textile industry is

one of the major contributions to the water pollution and causes major impact on available water quality through deliberate or inadvertent release of dye effluents into water bodies. Dyes have complex chemical structures that adhere to the surface of fabrics, thereby imparting colour to them. More than 100,000 chemically different dyes used in a wide variety of application such as textile [2], paper [3], tanning industries [4], plastic [5], printing [6], food processing [7], etc. Around 10,000 tons of synthetic dyes are used per year by textile industries alone, discharging nearly 100 tones of dyes in water bodies as effluents. As synthetic dyes are designed to resist breakdown with time and exposure to sunlight, water, soap, detergent and oxidizing agents [8, 9], they cannot be easily removed by conventional waste water treatment processes due to their complex structure and synthetic origin.

Methylene blue (MB), commercial dye used for various applications such as textile, papers, leathers, additives etc is heterocyclic aromatic compound having complex chemical structure and synthetic origin, owing to which it is resistant to biodegradation [10] and very stable to light [11] and oxidation [12]. This dye is highly carcinogenic, persisted, toxic and mutagenic in nature. Because of its cationic as well as aromatic nature it is easily soluble in aqueous or alcoholic medium and usually generates sulphur oxide and nitric oxide at higher temperature. On reduction, it reduces dissolved oxygen thereby modifies the

properties as well as characteristics of aqueous fluids and causes several damages to health such as breathing difficulties, nausea, vomiting, allergic dermatitis, skin irritation, cancer and mutations. Hence, for better environment, the removal of this noxious dye from aqueous environment is of a prime importance up to now several methods such as coagulation [13], biological treatment [14], chemical oxidation [15], membrane separation [16] and adsorption [17, 18] have been used to eliminate noxious dyes from aqueous environment. Amongst all these methods, adsorption provides attractive treatment due to its simplistic approach, economic consideration, greater efficiency and numerous benefits such as the capacity to remove dyes as a large scale, the ease of recovery and recyclability of adsorbents. Different classes of adsorbent such as activated carbon [19], polymeric materials [20], biomass [21], multiwall carbon nanotubes (MWCNT) [22] has been used to remove dyes from polluted water.

Conducting polymers attracted great interest in an academic and industrial level. The physical, chemical, electrical and optoelectric properties due to extended π - conjugated electron system make conducting polymers extensively explored materials. Conducting polymer such as polyphenylene, polypyrrole, polyacetylene, polythiophene and polyaniline have been extensively studied in multidisciplinary research areas like environment, electronics, electromagnetic, thermoelectric, sensors, batteries, electroluminescence and electrochemical application [23, 24, 25, 26, 27, 28]. Polyaniline is considered to be one of the most promising classes of organic conducting polymers due to its unique electrochemical properties, higher environmental stability, easy synthetic methodology, cost effectiveness, efficient thermal stability, and wide variety of applications has been most intensively investigated by researchers [29]. However, due to poor stability, poor mechanical properties, lower effective surface area, it is of limited use in environmental applications [30]. In order to

over their limitations, PANi is often polymerized in the presence of other materials to enhance its properties. Surface area and morphology plays an important role in increasing adsorption capacity of the polyanilinenanocomposite materials. Polyanilinenanocomposite have been widely used as adsorbent materials for the removal of dyes and other pollutants from waste water and hence, most favoured contender for various environmental applications [31].

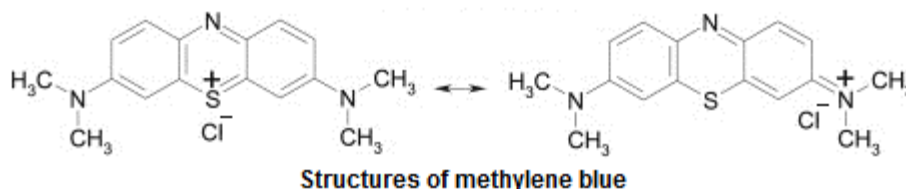
Graphene is one-atom-thick plane of graphite and due to its excellent thermal and electrical conductivity, exceptional electronic transport and excellent chemical tolerance capacities as well as its large surface-to-volume ratio, it has attracted research interest [32, 33, 34, 35, 35]. One of the most important features of graphene is its large theoretical specific surface area ($2630 \text{ m}^2\text{g}^{-1}$), which makes it a suitable adsorbent [36]. Because of these distinctive properties, it is often used for designing nanocompounds with polymers, metal organic frame work and metal nanoparticles etc [37, 38, 39, 40]. GOPAnin nanocomposites have showed enhanced physical and chemical properties compared with pure PANi or GO and have been exploited in many applications [41, 42, 43]. Besides GO, polyaniline based nanocomposites play a significant role in potential applications including photocatalytic, super capacitor, waste water treatment through adsorption etc owing to their low cost, facile synthesis, large surface area and physicochemical properties [44, 45, 46]. Various GO nanocomposite material with conducting polymers such as GO/polypyrrole, rGO/polypyrrole/Fe₃O₄ [47, 48] etc have been employed for the effective treatment of dye waste water.

Therefore, GOPAnin nanocomposites can be explored for the synthesis of nanocomposite materials to address the present day issue of water pollution.

In the present study we reported the hydrothermal synthesis of GOPAnin nanocomposites through a simple insitu oxidative polymerization technique for the adsorption of

cationic dye (MB). GO was synthesized by using modified Hummers method. Here grapheneoxide, due to the presence of oxygen containing functionalities, attains negative

charge where as polyaniline, due to presence of nitrogen containing functionalities (imine and amine), develops a positive charged backbone, thereby causing intensive electrostatic attraction between nanocomposites and dye molecules.



2. Experimental

Materials:

Graphite powder (99.9%), Potassium permanganate (99.9%), Sodium nitrate (99.9%), Aniline (99.5 %), Ammonium persulfate (99.5 %) are procured from E. Merck. Aniline was distilled and stored in the dark before use. All supplementary chemicals such as Benzoic acid, Sulphuric acid, Hydrochloric acid, Ethanol, acetone, Hydrogen peroxide were used are of analytical grade and solutions were prepared with doubly distilled water. Methylene Blue (MB) was purchased from Sigma-Aldrich and was used without further purification.

Synthesis of GO:

GO was synthesized using modified hummers method [49]. In three-neck round bottom flask (500 mL), 120 mL concentrated sulphuric acid was added. The flask was immersed in ice-bath under continuous stirring at 500 rpm. Five gram of Graphite powder was added into ice-cooled sulphuric acid. Subsequently 2.5 g NaNO_3 and 15 g KMnO_4 was added to it. After a while, the flask was removed from ice-bath and the reaction mixture was stirred over night. When light Grey paste was obtained, 150 mL of de-ionized water were added to dilute the paste. The diluted paste was heated to 98 °C by continuous stirring for 2 hours. Then 50 mL H_2O_2 were added and reaction mixture was stirred for 30 minutes. The reaction mixture was then filtered and washed

Preparation of Methylene Blue (MB) Solution:

weight 319.85. Scheme 1 shows its molecular structure. It is water soluble dye, which is blue in color with λ_{max} 664 nm [50]. Methylene blue

with 5% HCl until the filtrate becomes colorless. It was then washed with ethanol and subsequently with de-ionized water until the filtrate becomes neutral, and dried in an oven at 60 °C.

Preparation of GOPAninacomposite:

In 250 mL beaker, 2.3 g of prepared GO and doubly distilled Aniline (100 mL of 1M) were stirred for 18 hours for appropriate orientation of compounds. The Ammonium persulphate (100 mL of 1M) solution was then added slowly to the above mixture with continuous stirring at 30 °C. The whole reaction mixture was then transferred to Teflon inner container of the autoclave. The mixture was then diluted with de-ionized water up to 75% of the container. Teflon container was placed in hydrothermal autoclave and sealed with plumbing pliers. Autoclave was then transferred to oven, previously maintained at 125 °C. After 24 hours, autoclave was taken out of the oven and cooled at room temperature. The reaction mixture was centrifuged to get solid precipitate. The precipitate was washed with de-ionized water and ethanol to remove excess ions and monomers. The final product was dried in oven at 45 °C for 6 hours. This gave the bluish-black coloured GOPAni-1 composite with ratio 0.25:1. Similarly, other bluish-black coloured composite with ratio 0.50:1, 0.75:1 and 1:1 were prepared.

Methylene Blue has a molecular formula $\text{C}_{16}\text{H}_{18}\text{N}_3\text{ClS}$ with molecular (stock) solution was prepared by dissolving appropriate quantity in a volume of distilled water. The required solutions were prepared by

further diluting the stock solution with distilled water to get appropriate concentration.

Characterization technique:

The surface morphological study of the synthesized nanocomposite was carried out using JSM-6390 LV Scanning electron microscope (JEOL Ltd., Tokyo, Japan) operated at 10 kV, from Indian Institute of Technology, Varanasi, U.P., India. The size and shape of obtained GOPAni composites were studied using a PHILIPS-CM200 Transmission electron microscope operated at 20-200 kV, from Indian Institute of Technology, Mumbai, M.S., India. X-ray diffraction (XRD) pattern were recorded using X'PER PRO X-ray diffractometer (PAN analyzed) from $2\theta = 10^\circ$ to 90° using Cu- K α radiation at a scan rate 0.02 s⁻¹, from Vishvesvaraya National Institute of Technology, Nagpur, M.S., India. Fourier Transform Infrared (FTIR) spectra of the powdered nanocomposite were recorded using BRUKER-ALPHA FT-IR ATR spectrophotometer in the range of 600-4000 cm⁻¹ in spectral grade KBr plate, from Department of Chemistry, R.T.M. Nagpur University, Nagpur, M.S., India.

MB Adsorption Study:

The batch adsorption [51] study was carried out using MB dye in the water phase to investigate the adsorption ability of synthesized nanocomposite. Standard solutions of desired concentrations were prepared by diluting 1.0 g/L stock solution of MB. For adsorption, 0.25 g of GOPAni-1, GOPAni-2, GOPAni-3 and GOPAni-4 was added to 100 mL of different aqueous MB solutions having different concentrations ranging from 10 to 100 ppm (without adjusting pH). The solutions were stirred at constant speed of 300 rpm in continuous manner for 3 h. at $30 \pm 0.2^\circ\text{C}$. After equilibrium, dispersion was collected and filtered. The MB concentration was determined by monitoring absorbance at the maximum absorbency of MB (560 nm) using UV-VIS spectrophotometer (Shimadzu 1800). A calibration curve was prepared by plotting absorbance versus concentration and was used to determine the concentration of MB in the adsorption study.

The MB adsorption experiments were conducted at room temperature in a set of flasks by batch process to study the outcome of

different parameters such as type of adsorbent (GOPAni-1, GOPAni-2, GOPAni-3 and GOPAni-4), effect of contact time, effect of pH, and initial concentration of MB.

Effect of pH on MB removal

A series of 250mL flask were taken and each flask was added with 100 mL of MB solution at the concentration of 30 mg/L, (C_0). All the flasks were maintained at 30°C and pH of MB solution was varied in the range of 5.0 to 10.0 with the help of reagent grade 0.1 M sodium hydroxide and 0.1 M hydrochloric acid. In each flask 0.25 g of GOPAni composites were added and shaken on rotatory shaker (300rpm) for about three hours. After agitation, all the samples were filtered through whatman no. 42 filter paper. The final concentration of MB in each flask was determined spectrophotometrically. The percentage adsorption of MB in each case was determined from initial and final concentration of MB. In each case graph of percentage removal of MB versus pH was plotted. From the graph, optimum pH required for maximum adsorption of MB was obtained and this value of pH was used in the further studies.

Effect of adsorbent dose on MB removal

At optimum pH of 8 and temperature 30°C , all experiment as mentioned earlier were carried out with various amount of adsorbents (i.e. GOPAni-1, GOPAni-2, GOPAni-3 and GOPAni-4). The amount of adsorbent was varied from 0.7 to 4.0 g/L. In each case percentage adsorption was determined from initial and final concentration of MB in each flask. A graph of adsorbent dose in gram versus percentage removal of MB was plotted. From this graph maximum adsorbent dose was determined.

Effect of contact time on MB removal

The experiments were carried out at maximum pH (8), temperature (30°C) and by adding optimum adsorbent dose of GOPAni-1 (2.5 g), GOPAni-2 (2.0 g), GOPAni-3 (1.5 g) and GOPAni-4 (1.0 g). The contact time of MB on GOPAni composite was varied from 10 min to 180 min. The percentage adsorption of MB was calculated from initial and final concentration of MB. A graph of percentage removal of MB versus contact time was plotted. From this graph, optimum contact time for the maximum adsorption of MB was evaluated.

Effect of initial MB concentration

The experiments were carried out at the optimum, previously determined conditions, with the exception of concentration, MB. The concentration of MB in each case was a ranged from 10 mg/L to 100 mg/L. The percentage adsorption of MB was calculated from initial and final concentration of MB. A plot of percentage removal of MB versus concentration of MB was plotted. From this a maximum concentration of MB at which maximum percentage of adsorption took place was calculated.

Study of adsorption isotherm

The 100 mL of ten solutions of the concentration 10, 20, 30, 40, 50, 60, 70, 80, 90 and 100 mg/L were prepared by a proper dilution of stock solution of MB. All previously determined optimum parameters were used for studying the adsorption isotherm. The equilibrium concentration (C_e) in each case was determined from initial concentration (C_o), initial absorbance (A_o) and adsorption of solution after optimum time (A_t) as below;

$$C_e = \left(\frac{C_o}{A_o}\right) A_t \text{-----(1)}$$

In each case, amount of MB adsorbed (q_e) was evaluated by using the formula;

Langmuir equation related to the coverage of molecules on a solid surface to concentration of a medium above the solid surface at a fixed temperature. Langmuir equation is given in the subsequent form as;

$$q_e = \frac{q_{max} b C_e}{1 + b C_e} \text{-----(5)}$$

The Langmuir adsorption equation is frequently written in the following linear form as;

$$\frac{C_e}{q_e} = \frac{1}{q_{max} b} + \frac{C_e}{q_{max}} \text{-----(6)}$$

Where, q_e is the amount of solute adsorbed per unit weight of adsorbent (mg/g), C_e is the equilibrium concentration of solute in the bulk solution (mg/L), q_{max} is adsorption efficiency and also called as maximum monolayer adsorption capacity (mg/g) and 'b' is the adsorption energy. 'b' is the reciprocal of concentration at which half saturation of the adsorbent is reached.

$$q_e = \frac{(C_o - C_e) V}{m} \text{-----(2)}$$

Where, C_o (mg/L) is the initial concentration of MB, C_e is equilibrium concentration of MB, m is the mass of the adsorbent (GOPAni-composites) and V (mL) is the volume of MB solution.

Freundlich adsorption isotherm is capable of describing the adsorption of organic and inorganic compounds on the wide variety of adsorbents. The Freundlich adsorption equation can be written as;

$$\frac{x}{m} = q_e = k (C_e)^{1/n} \text{-----(3)}$$

Taking the logarithm of both sides,

$$\log q_e = \log k_f + \frac{1}{n} \log C_e \text{-----(4)}$$

Where, 'q_e' is equilibrium adsorption capacity (mg/g), C_e is the equilibrium concentration of dye in the solution (mg/L) and 'k_f' and 'n' are the constants incorporating all factors affecting the adsorption capacity and intensity of adsorption respectively.

From the above straight line equation and values of C_e and q_e , a plot of $\log q_e$ versus $\log C_e$ was plotted to verify the Freundlich adsorption isotherm.

From the above straight line equation and values of C_e and q_e obtained, another plot of ratio of C_e to q_e versus C_e was plotted to verify Langmuir adsorption isotherm.

The essential characteristic of Langmuir isotherm can be described by separation factor (R_L), which is given by the following equation;

$$R_L = \frac{1}{1 + b C_o} \text{-----(7)}$$

where, C_o (mg/L) is the initial concentration of the dye solution.

The value of separation factor (R_L), indicates the shape of the isotherm and nature of adsorption process to be either unfavorable ($R_L > 1$), Linear ($R_L = 1$), favorable ($0 < R_L < 1$) or irreversible ($R_L = 0$).

3. Results and Discussion

Fourier Transform Infrared Spectral Analysis

Fig.1 shows the FT-IR spectra of graphene oxide, PANi and GOPAni nanocomposites. The peak at 3740, 3362 and 1503-1028 cm^{-1}

for graphene oxide are attributed to the OH, C=O in COOH and C-O in COH/COC (epoxy) functional groups respectively [52,53,54]. Compared with the peaks of graphene oxide, the C=O Peak for GOPAni is downshifted to 1545-1569 cm^{-1} ; the peaks of C-O in COH/COC (epoxy) are also red-shifted clearly. These indicate the carboxyl groups from graphene oxide are linked on the nitrogen of PANi backbone. The spectral red- shift

phenomena of chemically synthesized nanocomposite result from the π - π interaction and hydrogen bonding between the graphene oxide and PANi. Besides, there are large amount of oxygenous groups in the graphene oxide, which can easily interact with the nitrogen atoms in the -NH- group of PANi backbone through -OH...N- and -O...H-N- hydrogen bonds.

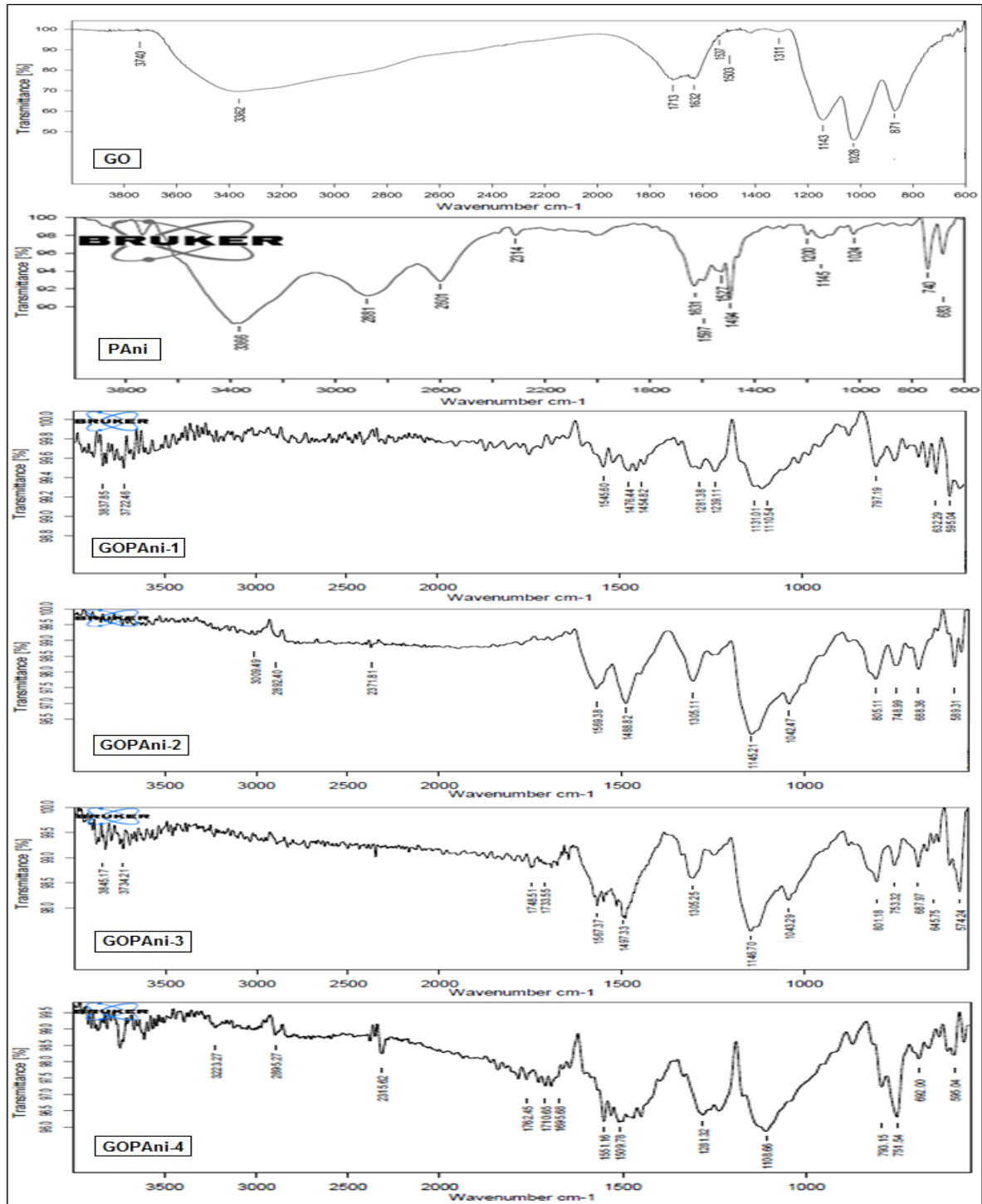


Fig. 1 FTIR spectra of PANi, GO, GOPAni-1, GOPAni-2, GOPAni-3 and GOPAni-4 nanocomposites

From the Fig. 1, it was also found that PANi existed in the composites owing to vibrational signals on benzoids and quinoids rings at 1537 cm^{-1} and 1503 cm^{-1} respectively [55]. The other signals found where at 3837.85 cm^{-1} , 3722.46 cm^{-1} , 3540 cm^{-1} , 3845.17 cm^{-1} and 3580 cm^{-1} due to the N-H stretching mode, the peak at 2800 cm^{-1} , 2892.40 cm^{-1} , 2883 cm^{-1} and 2895.27 cm^{-1} are due to the C-H bond.

The peaks observed at 1545.60 cm^{-1} , 1569.38 cm^{-1} , 1567.37 cm^{-1} and 1551.16 cm^{-1} are due to the benzoid ring respectively, similarly the peaks obtained in composites at 1476.44 cm^{-1} , 1488.82 cm^{-1} , 1497.33 cm^{-1} and 1509 cm^{-1} are due to quinoid structure respectively. The peaks appeared at 1454.82 cm^{-1} , 1450 cm^{-1} , 1350.50 cm^{-1} and 1440.25 cm^{-1} are due to the -N=Quinoid=N- . The peaks obtained in the figure at 1131.01 cm^{-1} , 1145.21 cm^{-1} , 1146.70 cm^{-1} and 1108.66 cm^{-1} are ascribed to C-N+.

The major peaks for PANi in the spectrum of composites belongs to C-H vibration, C-N vibration, C=C vibration and C=N vibration and which are found in literature [56]. The initial peak in GOPAni such as 624 cm^{-1} is due to aromatic ring deformation. The shift in GOPAni C-H, C-N, C=C and C=N vibrations are visible due to Graphene-polyaniline interaction

It was observed that GOPAninocomposites shows similar peak to PANi and the peak intensities are also close to PANi. No additional peak is observed which indicates that crystal structure of PANi is maintained in the GOPAninocomposites.

For GOPAninocomposites, no GO peak is observed in the results and it is completely missing in GOPAni-1, GOPAni-2, GOPAni-3 and GOPAni-4. It reveals that the

layer of GO are completely exfoliated. This exfoliation of GO layer helps to align the PANi chains and enhance the crystalline nature of GOPAninocomposites.

X-ray diffraction analysis

Figure.2 depicts the x-ray diffraction pattern of the GO, PANi and samples of hydrothermally synthesized GOPAni-1, GOPAni-2, GOPAni-3 and GOPAni-4 nanocomposites. The XRD pattern of GO illustrated an intense and sharp peak centred at $2\theta = 20^\circ$, which corresponds to the inter planner spacing of GO sheets. The observed 2θ for GO could be attributed to the (001) reflection plane, which is due to the process of synthesis and layers of water within inter planner space of GO [34, 42]. It is evident from Figure 2, the PANi exhibited diffraction peaks at 2θ value 20° and 25° , which are characteristic, peaks of PANi. These peaks indicate the crystalline nature of PANi [57]. The peaks at angle 2θ values of 20° and 25° shows the periodic repetition of benzoid and quinoid rings in PANi chains [58]. As per the XRD pattern of GOPAni-1, GOPAni-2, GOPAni-3 and GOPAni-4, the peak of GO has been reduced indicating that aggregation of GO diminished and was utilized by PANi to produce a nanocomposites material [42]. Characteristic GO and PANi peaks can be seen clearly in the XRD spectrum of GOPAni-1, GOPAni-2, GOPAni-3 and GOPAni-4, which proves the uniform occurrence of GOPAninocomposites. The peak at 20° becomes prominent as the concentration of GO increases in the nanocomposites. It is the indication of strong interaction of GO with benzene ring of PANi. Therefore, XRD investigation established the successful synthesis of GOPAninocomposites and crystalline nature of these composites.

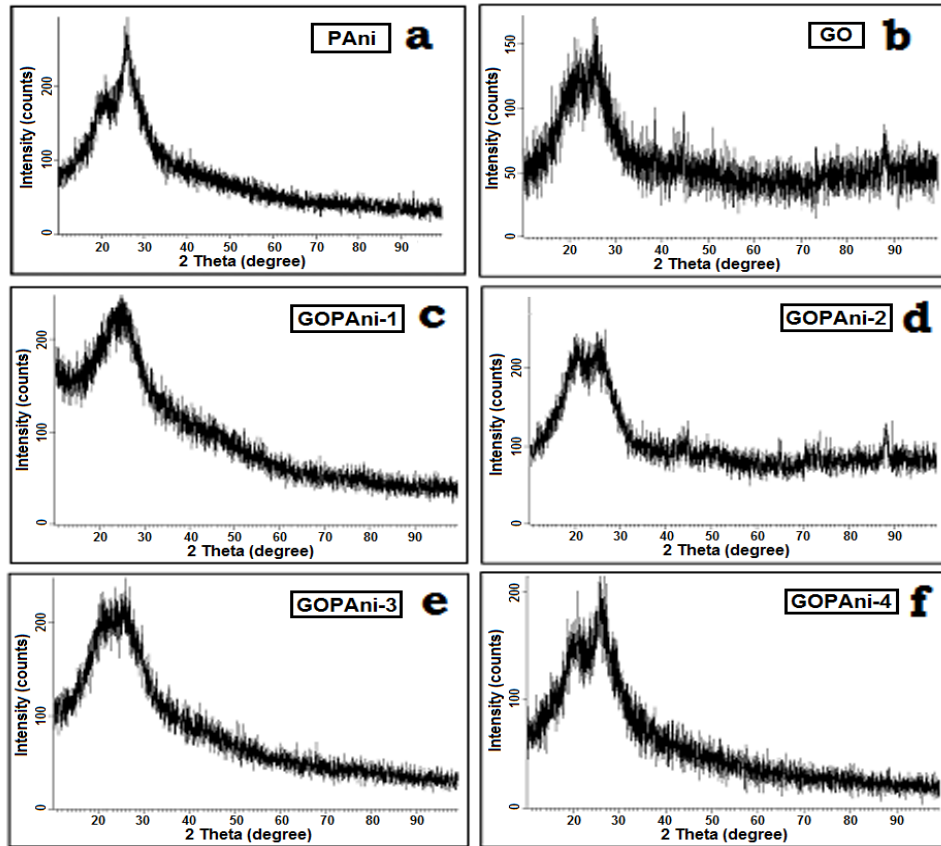


Fig. 2 XRD spectrum of PANi (a), GO (b), GOPAni-1 (c), GOPAni-2 (d), GOPAni-3 (e) and GOPAni-4 (f) nanocomposites

Scanning electron microscopy

The SEM images of PANi, GO and GOPAni composites are shown in Fig. 3. It reveals

multilayer structure of GO with stack sheets and rod like structure of PANi.

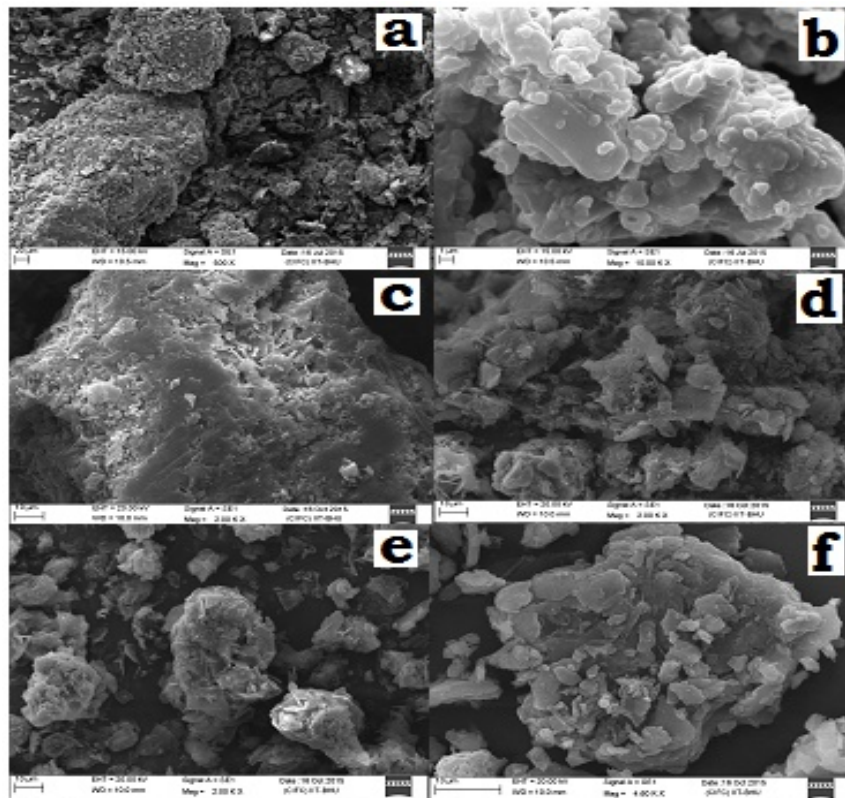


Fig. 3 SEM micrographs of PANi (a), GO (b), GOPAni-1 (c), GOPAni-2 (d), GOPAni-3 (e) and GOPAni-4 (f) nanocomposites

It can be seen that the morphology of GOPAninano composites is different from that of PANi and GO. GOPAninano composites show multiple shapes. The morphology is like flakes with fibres. The polymerization of aniline has been take place on the GO surface and

results in flaky structures. The dispersion of GO in PANimatrix takes place in nanocomposites.

Transmission electron microscopy

The morphological structure of nanocomposites was established by transmission electron microscopy.

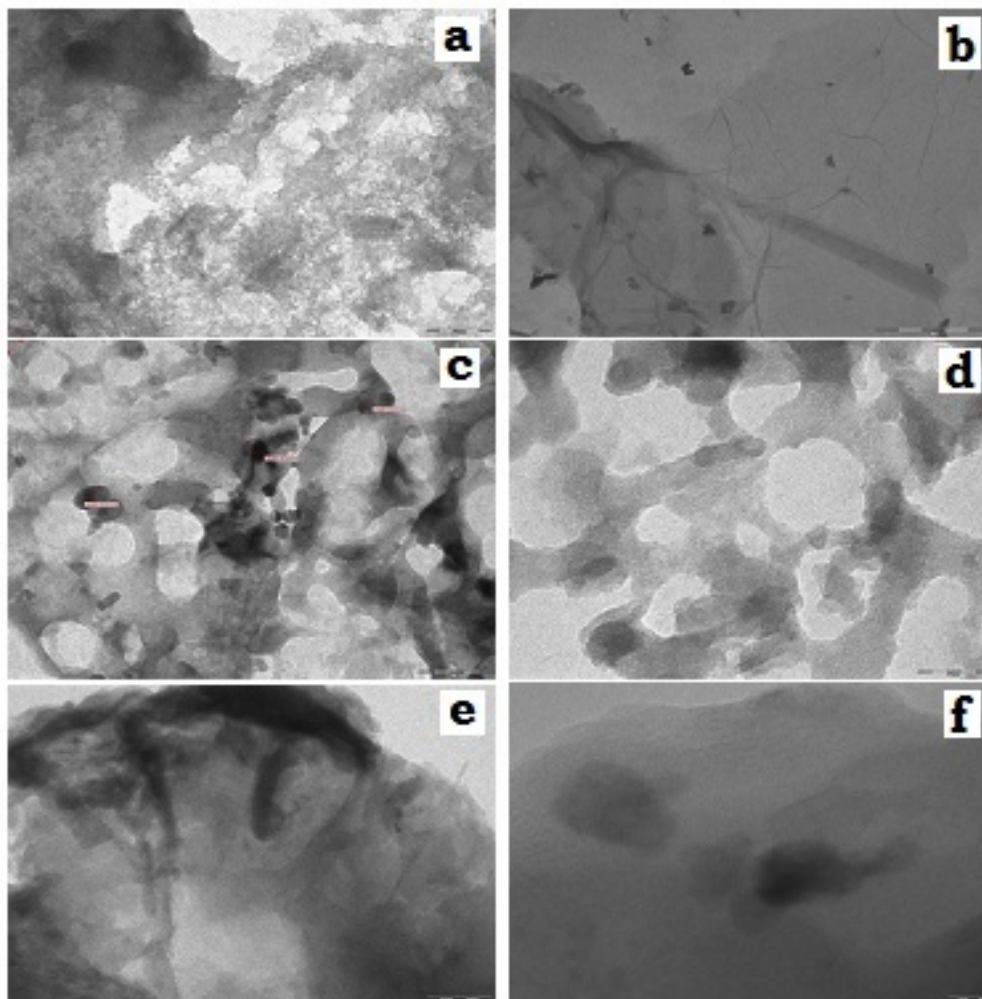


Fig. 4 TEM Images of PANi (a), GO (b), GOPAni-1 (c), GOPAni-2 (d), GOPAni-3 (e) and GOPAni-4 (f) nanocomposites

Fig. 4 Shows the TEM images of PANi, GO and GOPAninano composites. The morphology of pure PANi shows the tubular structure. However, the images obtained for GOPAni-1, GOPAni-2, GOPAni-3 and GOPAni-4 with different concentration of GO, shows different morphology from PANi. This may be attributed to polymerization of aniline in presence of GO sheets. It is noted that GO get distributed in PANi and agglomeration of GO does not takes place.

The sizes of some molecules of nanocomposites are in range of 100-500 nm with tubular PANi structure differed substantially among individual tubes of diameter in the range

50-200 nm and lengths 1-50 mm. [59]. TEM images also revealed morphological features and characteristics of GOPAni composites. TEM image indicates that a surface morphology of GOPAninano composite was irregular surface which is responsible for adsorption of MB.

Adsorption studies

Effect of pH of solution:

Generally the pH is an important factor affecting adsorption [60]. Many workers have suggested the pH dependency of dyes binding process on different materials [61, 62, 63, 64, 65]. The efficiency of adsorption is depends on solution pH, since variation in pH leads to the variation in degree of ionization of dye

molecule and surface property of adsorbent [66, 67]. Therefore, the removal of MB by GOPAni composites was examined at different pH value ranging from 5 to 10 at 30°C (50 mg of MB per Litre and equilibrated for three hours) and

results are shown in Fig. 5. It is evident from the figure that all GOPAni adsorb MB dye in the higher pH value while the percentage removal of MB increases by increasing the pH value

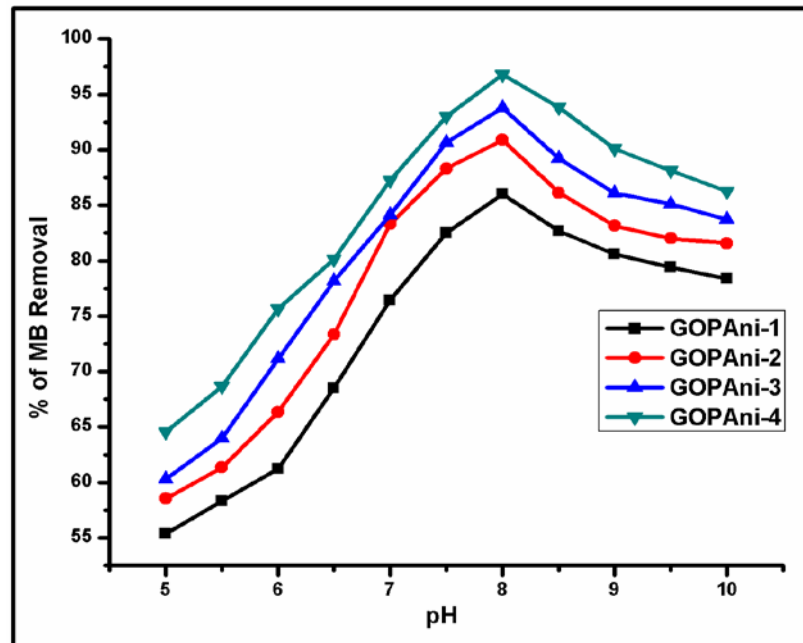


Fig. 5 Effect of pH on MB removal by GOPAni-1, GOPAni-2, GOPAni-3 and GOPAni-4 nanocomposites

The results indicate that the composite show increasing removal capacity in pH 5.0 to 7.5. At pH 8.0, the removal of MB is maximum for all the composite. Further increase in pH up to 10, capacity decreases [68]. The percentage removal of MB for GOPAni-1, GOPAni-2, GOPAni-3 and GOPAni-4 are 86.02%, 90.98%, 93.77% and 96.78% respectively. The removal by composites is in the following order,

$$\text{GOPAni-1} < \text{GOPAni-2} < \text{GOPAni-3} < \text{GOPAni-4}$$

At higher pH(>8), the percentages removal found to decrease because the surface that the removal efficiencies of GOPAni-1 and GOPAni-2 were 85.98% and 90.41% respectively at 180 min by addition of 2.5 g/L and 2.0 g/L of GOPAni-1 and GOPAni-2 while removal efficiencies of GOPAni-3 and GOPAni-4 were found to be 93.55% and 96.42% respectively at 180 min by addition of 1.5 g/L and 1.0 g/L of GOPAni-3 and GOPAni-4 respectively.

area of the composite was more protonated and competitive adsorption takes place between H^+ and MB^+ ions. Therefore, H^+ ions react with $-\text{COO}^-$ groups on the surface of composites and results in blocking of the number of adsorbing sites for removal of MB.

Effect of adsorbent dose

Effect of adsorbent dose on adsorption of MB dye was varied by changing the adsorbent dose from 0.7 g/L to 4.0 g/L with 50 mg/L MB solution. It was observed

In all the cases after addition of higher dose of respective adsorbents, the removal efficiency almost remains constant [69]. The effect of adsorbent upon removal of MB is shown in Fig. 6. The adsorption capacity of GOPAni composites are compared with other adsorbents for removal of MB and are presented in Table.1.

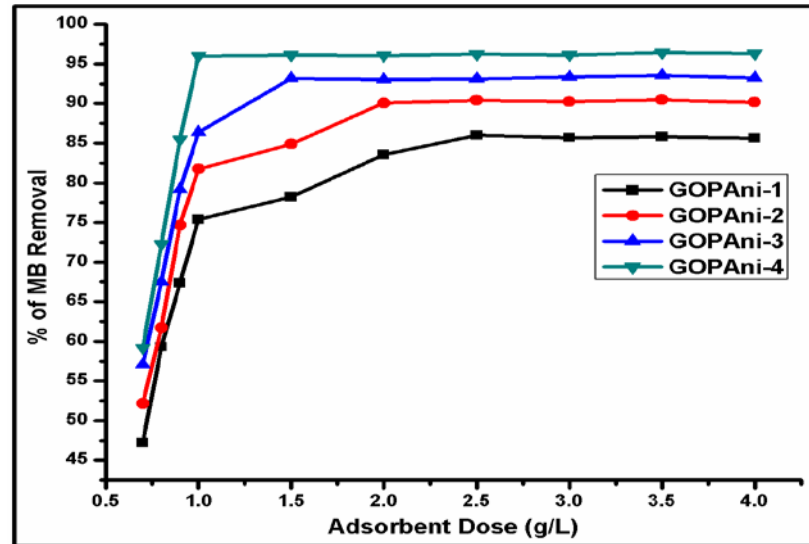


Fig. 6 Effect of Adsorbent dose on MB removal by GOPAni-1, GOPAni-2, GOPAni-3 and GOPAni-4 nanocomposites

Table.1 Comparison of GOPAni composites with other adsorbents for removal of Methylene blue dye. (adsorption capacity, mg/g).

Adsorbents	Adsorption capacity(q_m)	References
Acid activated bentonite	20.16	[70]
Clay	58.2	[71]
Charcoal	62.7	[72]
Activated carbon	9.81	[73]
Pyrolysed furniture	80	[74]
Pitch	33	[75]
Activated date pits	12.9	[76]
Coir pith carbon	5.87	[77]
Zeolite	53.1	[78]
Amorphous silica	22.66	[79]
Raw kaolin	13.99	[80]
Glass wool	2.24	[81]
Posidoniaoceanica fibres	5.56	[82]
Living biomass	1.17	[83]
Coal fly ash	12.7	[84]
Fly ash (CFA)	6.04	[85]
Red mud	2.49	[86]
Coconut husk	99	[87]
Coffee husks	90.1	[88]
Walnut sawdust	59.17	[89]
Rice husk	40.59	[90]
Cotton waste	24	[91]
Orange peel	18.6	[92]
Wheat shells	16.56	[93]
GOPAni-1	24.89	Present study
GOPAni-2	31.34	Present study
GOPAni-3	42.51	Present study
GOPAni-4	64.15	Present study

Effect of Contact Time:

The equilibrium time between the adsorbate and the adsorbent is of great importance in the removal of dyes by adsorption. For an adsorbent to be efficient in removal of dye, it needs to be able to a rapid uptake of the dye and reach the equilibrium in

short time. Adsorption equilibrium time is determined as the time after which the uptake of the dye solution remained unchanged during the course of adsorption process. Fig.7 shows the effect of contact time on the percentage removal of MB by GOPAni composites.

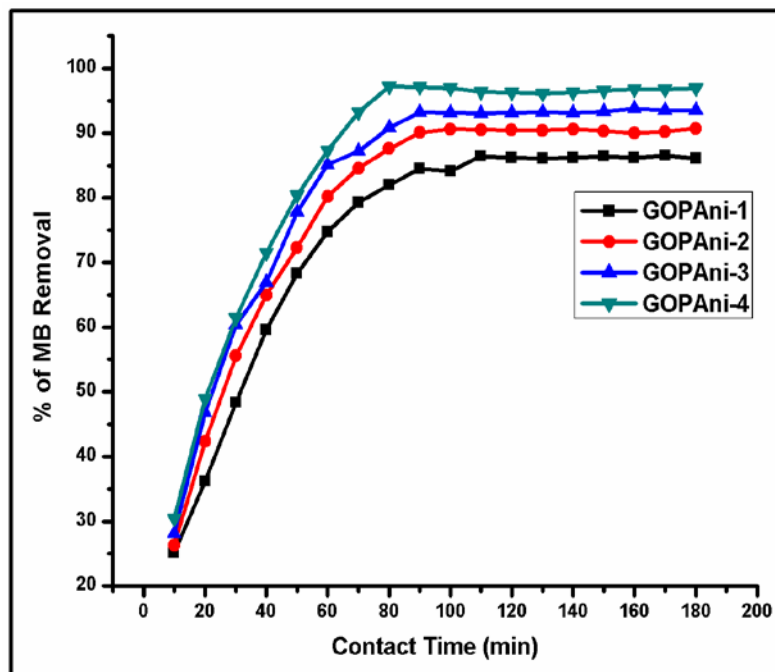


Fig. 7 Effect of Contact time on MB removal by GOPAni-1, GOPAni-2, GOPAni-3 and GOPAni-4 nanocomposites

It can be seen that in all the nanocomposites, at initial stage percentage removal of MB was fast and then becomes slow and gets stagnated with increase in time. In case of GOPAni-1 and GOPAni-2, percentage adsorption of MB increases from 25.13% to 86.42% and 26.33% to 90.62% respectively, by increasing the contact time from 10 min to 110 min and 100 min. Beyond this time it almost remain constant in both the cases.

In case of GOPAni-3 and GOPAni-4, the percentage removal increases from 28.14% to 93.22% and 30.45% to 97.22% respectively, by varying the contact time from 10 min to 90 min and 80 min. Further increase in contact

After maximum contact time ability of each composite to adsorb MB almost remains constant. This is due to complete saturation of MB on all the surface active sites [94, 95, 96, 97].

time does not increase the adsorption. The order of contact time for rate of removal of MB by GOPAni composites is,

GOPAni-1 (110 min) > GOPAni-2 (100 min) > GOPAni-3 (90 min) > GOPAni-4 (80 min)

The result shows that as the amount of GO increases in the composite, the contact time decreases. This is due to availability of more surface area and active sites for the adsorption of MB. Initial increase in the percentage of adsorption is due to the filling of active sites on the adsorbents (composites). At each optimum time, almost all the active sites on the composites are full of MB molecules. The amount of MB adsorbed by nanocomposites and it remained in the solution are in equilibrium.

Effect of initial dye concentration

The effect of initial dye concentration plays a significant role in the amount of dye adsorbed, and percentage dye removal. It depends on the immediate relation between the concentration of dye and available sites on the

adsorbed surface. The initial concentration of adsorbate in solution provides an important driving force in overcoming mass transfer resistance between the aqueous and solid phase [98, 99]. Equilibrium adsorption studies was performed and the equilibrium is established when the concentration of MB dye in the solution is in dynamic balance with that of surface of GOPAni composites. Effect of initial concentration on removal of MB was studied at different initial concentrations of MB (10mg/L to 100 mg/L) keeping all other parameters constant. The results are shown in Fig.8. The percentage of removal was varied according to the initial concentration of MB. It indicates that the initial MB concentration has an important influence on the adsorption capacity of GOPAni composites. At low concentration (10mg/L), maximum percentage removal was found to be 89.34% (GOPAni-1), 91.91% (GOPAni-2), 95.08% (GOPAni-3) and 97.07% (GOPAni-4) respectively. Increasing the concentration to 50 mg/L, the percentage removal was observed to be 83.69% (GOPAni-1), 86.26% (GOPAni-2), 88.43% (GOPAni-3), and 90.42% (GOPAni-4).

However, further increase in concentration to 100mg/L, the percentage removal further decreases to 54.82% (GOPAni-1), 56.39% (GOPAni-2), 59.56% (GOPAni-3), and 60.55% (GOPAni-4) respectively.

The enhanced removal at low concentration could be due to faster movement of MB molecules in to the activated sites of the GOPAni composites. However, in higher concentration (100 mg/L) the percentage removal decreased due to saturation of absorption sites on the GOPAni surface. It may also be attributed to intraparticle diffusion of MB molecules to composite sites. In addition, steric repulsion between the solute molecules could slow down the adsorption process and thereby decreases the removal [100,101]. At lower concentrations, all MB present in the adsorption medium could interact with the binding sites on the surface of adsorbent [102, 103]. So, higher removal was obtained. Besides lower removal were observed at higher concentrations because of the saturation of the adsorption sites have take place [104].

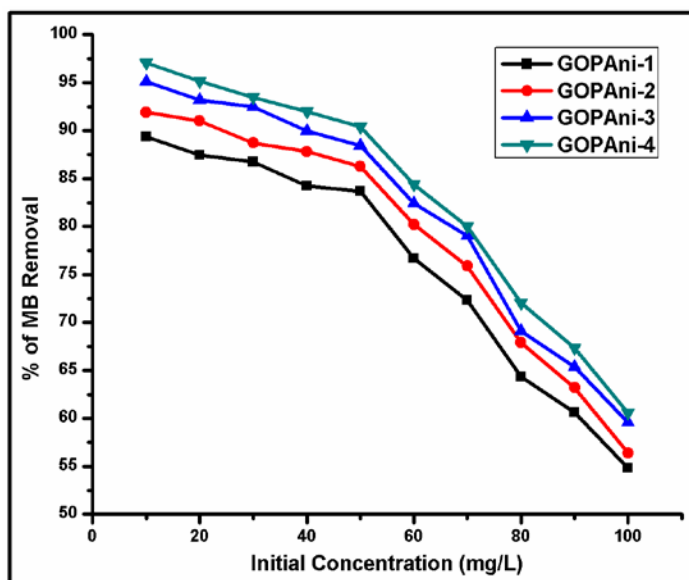


Fig. 8 Effect of Contact time on MB removal by GOPAni-1, GOPAni-2, GOPAni-3 and GOPAni-4 nanocomposites

Adsorption isotherm

In order to establish the most appropriate correlation for an equilibrium data in the design of adsorption system, two common isotherm models were tested: Freundlich and Langmuir models. The applicability of the isotherm equations were compared by judging the square of correlation

coefficient (R^2) [105, 106, 107, 108, 109, 110, 111].

Freundlich isotherm:

At a fixed adsorbent dose, different initial concentration of adsorbate was taken for equilibrium studies. Different adsorption isotherms were tested for the adsorption

process. It was found that the data fitted well into linearised Freundlich adsorption isotherm whose mathematical expression is given in equation (4). The Freundlich equation suggests multilayer adsorption. Adsorption energy exponentially decreases on completion of the adsorption centers of an adsorbent. The plot of $\log q_e$ versus $\log C_e$ for GOPAni-1, GOPAni-2, GOPAni-3 and GOPAni-4 (Fig.9.) shows a linear curve and hence the adsorption obeys Freundlich isotherm.

Therefore, the parameters of k_f and 'n' were be estimated from the intercept and slope of the plots $\log q_e$ versus $\log C_e$. The calculated parameters at 30°C were presented in Table.2. The k_f values of all the adsorbents i.e. GOPAni-1, GOPAni-2, GOPAni-3 and GOPAni-4 were found to be 4.789, 7.140, 11.501 and 19.923 mg/g respectively, and

indicates dominance of adsorption capacity. The Freundlich exponent 'n' were 2.170, 2.310, 2.533 and 2.743 for GOPAni-1, GOPAni-2, GOPAni-3 and GOPAni-4 respectively, and indicates the favourable adsorption.

The square of the correlation coefficient (R^2) values are 0.945, 0.941, 0.949 and 0.958 for GOPAni-1, GOPAni-2, GOPAni-3 and GOPAni-4 respectively, and shows well fitting of the Freundlich isotherm. The 'n' values are in between 1 to 10 and indicates the favorable adsorption of MB on GOPAni-1, GOPAni-2, GOPAni-3 and GOPAni-4 (Table.2). The values of k_f clearly show the dominance of adsorption capacity. The intensity of adsorption (n) is indicative of the bond energies between MB and composites as well as the possibility of slight chemisorption rather than physisorption.

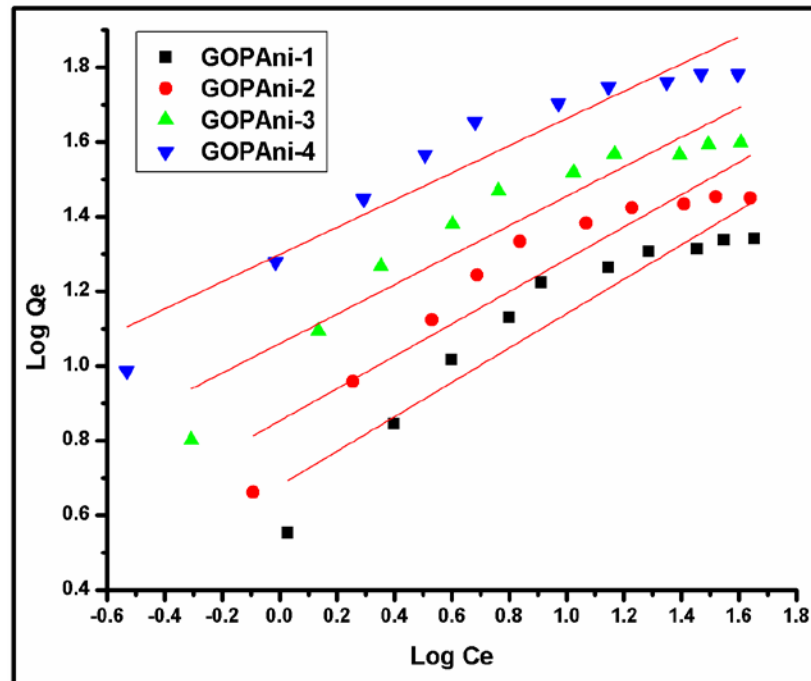


Fig. 9 Plot of Freundlich Adsorption Isotherm for GOPAni-1, GOPAni-2, GOPAni-3 and GOPAni-4 nanocomposites

Langmuir Isotherm:

The Langmuir adsorption isotherm suggests that, when the adsorbate occupies site, further adsorption cannot take place at that site. All the sites are energetically equivalent and there is no interaction between molecules adsorbed on the neighboring sites [112]. The equilibrium data also well fitted in Langmuir linear plot of C_e/q_e versus C_e and it suggests the applicability of Langmuir isotherms. The values

of adsorption efficiency q_{max} and adsorption energy 'b' were determined from the slope and intercept of the plots shown in Fig.10. The Langmuir monolayer adsorption capacity q_{max} gives the amount of the adsorbate required to occupy all the available sites per unit mass of the sample.

The values of q_{max} for GOPAni-1, GOPAni-2, GOPAni-3 and GOPAni-4 were found to be 24.899, 31.342, 42.518 and 64.157

mg/g while values of 'b' were 0.185, 0.254, 0.341 and 0.455 respectively are presented in Table.2. This lower value of 'b' indicates the

affinity between solute and adsorbent site which rules out the possibility of chemisorptions.

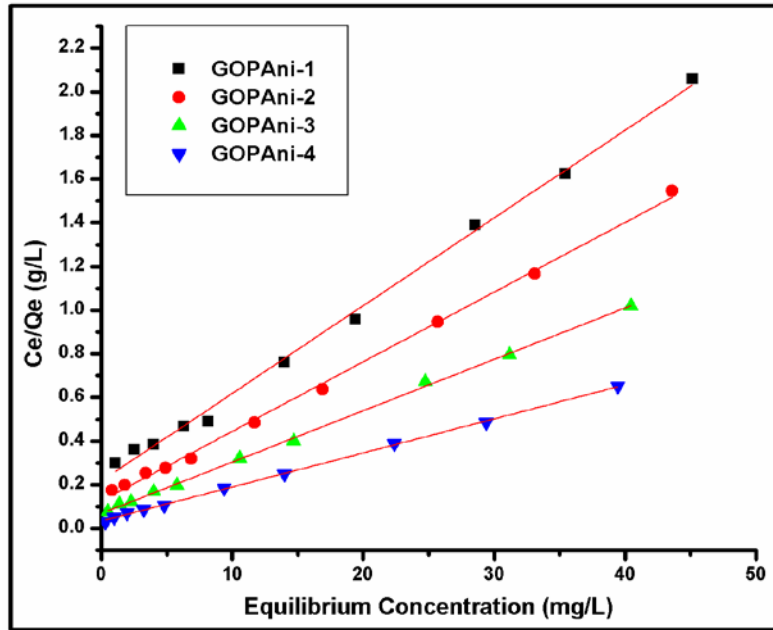


Fig. 10 Plot of Langmuir Adsorption Isotherm for GOPAni-1, GOPAni-2, GOPAni-3 and GOPAni-4 nanocomposites

To confirm the adsorbability of the adsorption process, the equilibrium parameter also called separation factor (R_L) was computed for GOPAni-1, GOPAni-2, GOPAni-3 and

GOPAni-4 and found to be fractional in the range of 0 to 1, indicating that the adsorption process is favorable for these adsorbents for the removal of MB dye (Fig.11).

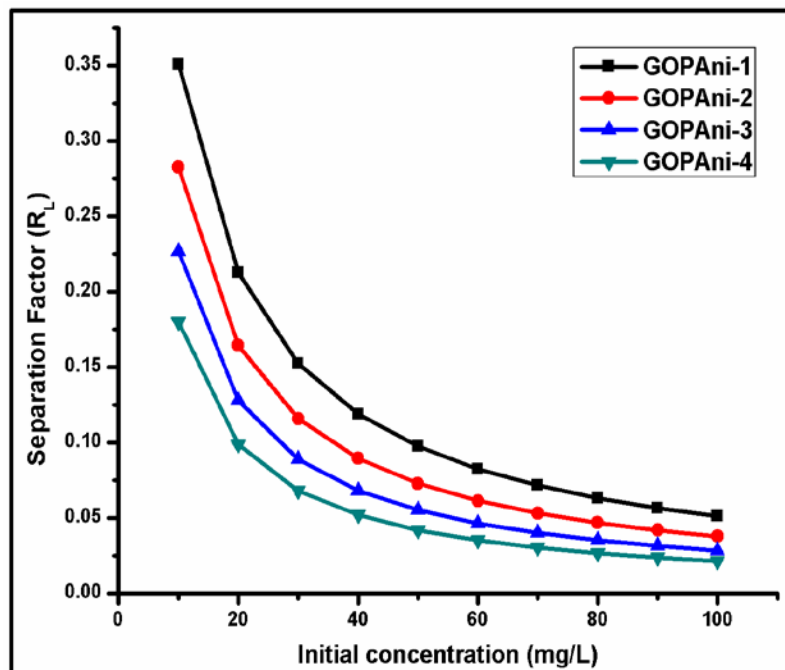


Fig. 11 Plot of Separation Factor vs. Initial MB Concentration for GOPAni-1, GOPAni-2, GOPAni-3 and GOPAni-4 nanocomposites

Table.2: Freundlich and Langmuir isotherm parameters for adsorption of MB dye on GOPAni-1, GOPAni-2, GOPAni-3 and GOPAni-4 adsorbents

Adsorbent	Freundlich Isotherm Parameter			Langmuir Isotherm Parameter		
	R ²	n	k _f	R ²	b	Q _m
GOPAni-1	0.945	2.170	4.789	0.999	0.185	24.899
GOPAni-2	0.941	2.310	7.140	0.999	0.254	31.342
GOPAni-3	0.949	2.533	11.501	0.999	0.341	42.518
GOPAni-4	0.958	2.743	19.923	0.999	0.455	64.157

The correlation coefficients of the Langmuir model were higher than that of Freundlich model suggesting further resembling monolayer adsorption process. This adsorption study indicates that experimental results have been significantly fitted Langmuir adsorption systems.

4. Conclusion

GOPAni nano composites have been hydrothermally synthesized by a simple in situ oxidative polymerization technique. The equilibrium studies for the adsorption of MB dye from aqueous solution on to GOPAni nano composites were studied with variation in MB concentration. The uptake of the dye was studied using UV-Visible spectroscopy. The removal efficiency of MB was found to be pH dependent with maximum dye adsorption at pH 8. It is seen that MB adsorption onto nanocomposites is much more noticeable than the other adsorbents (Table.1). Adsorption rate increases in the following order; GOPAni-1 < GOPAni-2 < GOPAni-3 < GOPAni-4. This is probably due to the increase in surface area of nanocomposite substrates.

5. References

- [1] Sen, T.K., Afroze, S., Ang, H. 2011. Equilibrium, kinetics and mechanism of removal of methylene blue from aqueous solution by adsorption onto pine cone biomass of pinus radiata. *Water Air Soil Pollut.* 218: 499-515.
- [2] Sokolowska-Gajda, J., Freeman, H.S., Reife, A. 1996. Synthetic dyes based on environmental considerations. Part 2: Iron complexes formazan dyes. *Dyes Pigment.* 30: 1-20.
- [3] Ivanov, K., Gruber, E., Schempp, W., Kirov, D. 1996. Possibilities of using zeolite as filler and carrier for dyestuffs in paper. *Papier* 50: 7-8.
- [4] Kabdasli, I., Tunay, O., Orhon, D. 1999. Wastewater control and management in a leather tanning district. *Water Sci. Technol.* 40: 261-267.
- [5] Bensalah, N., Alfaro, M.Q., Martínez-Huitle, C. 2009. Electrochemical treatment of synthetic wastewaters containing alizarin dye. *Chem. Eng. J.* 149: 348-352.
- [6] Dawood, S., Sen, T.K., Phan, C. 2014. Synthesis and characterisation of novel-activated carbon from waste biomass pine cone and its application in the removal of congo red dye from aqueous solution by adsorption. *Water Air Soil Pollut.* 225: 1-16.
- [7] Yagub, M.T., Sen, T.K., Afroze, S., Ang, H.M. 2014. Dye and its removal from aqueous solution by adsorption: A review. *Adv. Colloid Interface Sci.* 209: 172-184.
- [8] Chequer, F.M.D., de Oliveira, D.P., Ferraz, E.R.A., de Oliveira, G.A.R., Cardoso, J.C., Zanoni, M.V.B. 2013.

- Textile Dyes: Dyeing Process and Environmental Impact; InTech Open Access Publisher: Rijeka, Croatia.
- [9] Couto, S.R. 2009. Dye removal by immobilised fungi. *Biotechnol. Adv.* 27: 227-235.
- [10] Shahabuddin, S., Sarih, N.M., Ismail, F.H., Shahid, M.M., Huang, N.M. 2015. Synthesis of chitosan grafted-polyaniline/ Co_3O_4 nanocubenanocomposites and their photocatalytic activity toward methylene blue dye degradation. *RSC Adv.* 5: 83857-83867.
- [11] Aksu, Z. 2005. Application of biosorption for the removal of organic pollutants: A review. *Process Biochem.* 40: 997-1026.
- [12] Shahabuddin, S., MuhamadSarih, N., Mohamad, S., JoonChing, J. 2016. SrTiO_3 nanocube-doped polyanilinenanocomposites with enhanced photocatalytic degradation of methylene blue under visible light. *Polymers.*
- [13] Papic, S., Koprivanac, N., Bozic, A.L., Metes, A. 2004. Removal of some reactive dyes from synthetic wastewater by combined Al (III) coagulation/carbon adsorption process. *Dyes Pigment.* 62: 291-298.
- [14] Gonzalez-Gutierrez, L.V., Escamilla-Silva, E.M. 2009. Reactive red azo dye degradation in a UASB bioreactor: Mechanism and kinetics. *Eng. Life Sci.* 9: 311-316.
- [15] Zou, H., Ma, W., Wang, Y. 2015. A novel process of dye wastewater treatment by linking advanced chemical oxidation with biological oxidation. *Arch. Environ. Prot.* 41: 33-39.
- [16] Akbari, A., Remigy, J., Aptel, P. 2002. Treatment of textile dye effluent using a polyamide-based nanofiltration membrane. *Chem. Eng. Processing* 41: 601-609.
- [17] Haldorai, Y., Shim, J. J. 2014. An efficient removal of methyl orange dye from aqueous solution by adsorption onto chitosan/MgO composite: A novel reusable adsorbent. *Appl. Surf. Sci.* 292, 447-453.
- [18] Mahto, T.K., Chandra, S., Haldar, C., Sahu, S.K. 2015. Kinetic and thermodynamic study of polyaniline functionalized magnetic mesoporous silica for magnetic field guided dye adsorption. *RSC Adv.* 5: 47909-47919.
- [19] HosseiniKoupale, E., AlaviMoghaddam, M., Hashemi, S. 2013. Successful treatment of high azo dye concentration wastewater using combined anaerobic/aerobic granular activated carbon-sequencing batch biofilm reactor (GAC-SBBR): Simultaneous adsorption and biodegradation processes. *Water Sci. Technol.* 67: 1816-1821.
- [20] Hu, J., Song, Z., Chen, L., Yang, H., Li, J., Richards, R. 2010. Adsorption properties of MgO (111) nanoplates for the dye pollutants from wastewater. *J. Chem. Eng. Data* 55: 3742-3748.
- [21] Valix, M., Cheung, W.H., McKay, G. 2009. Sulfur fixation on bagasse activated carbon by chemical treatment and its effect on acid dye adsorption. *Adsorption* 15: 453-459.
- [22] Ma, J., Yu, F., Zhou, L., Jin, L., Yang, M., Luan, J., Tang, Y., Fan, H., Yuan, Z., Chen, J. 2012. Enhanced adsorptive removal of methyl orange and methylene blue from aqueous solution by alkali-activated multiwalled carbon nanotubes. *ACS Appl. Mater. Interfaces* 4: 5749-5760.
- [23] Bairi, V.G., Bourdo, S.E., Sacre, N., Nair, D., Berry, B.C., Biris, A.S., Viswanathan, T. 2015. Ammonia gas sensing behavior of tanninsulfonic acid doped polyaniline- TiO_2 composite. *Sensors* 15: 26415-26429.
- [24] Sengodu, P., Deshmukh, A.D. 2015. Conducting polymers and their inorganic composites for advanced Li-ion batteries: A review. *RSC Adv.* 5: 42109-42130.
- [25] Hu, Z., Zu, L., Jiang, Y., Lian, H., Liu, Y., Li, Z., Chen, F., Wang, X., Cui, X. 2015. High specific capacitance of polyaniline/mesoporous manganese dioxide composite using $\text{K}_2\text{H}_2\text{SO}_4$ electrolyte. *Polymers* 7: 1939-1953.
- [26] Bhadra, S., Khastgir, D., Singha, N.K., Lee, J.H. 2009. Progress in preparation, processing and applications of polyaniline. *Prog. Polym. Sci.* 34: 783-810.
- [27] Shih, H.K., Chen, Y.H., Chu, Y.L., Cheng, C.C., Chang, F.C., Zhu, C.Y., Kuo, S.W. 2015. Photo-crosslinking of pendent uracil units provides supramolecularhole injection/transport

- conducting polymers for highly efficient light-emitting diodes. *Polymers* 7: 804-818.
- [28] Baharin, S.N.A., MuhamadSarih, N., Mohamad, S., Shahabuddin, S., Sulaiman, K., Ma'amor, A. 2016. Removal of endocrine disruptor di-(2-ethylhexyl)phthalate by modified polythiophene-coated magnetic nanoparticles: Characterization, adsorption isotherm, kinetic study, thermodynamics. *RSC Adv.* 6: 44655-44667.
- [29] Boeva, Z.A., Sergeev, V. 2014. Polyaniline: Synthesis, properties, and application. *Polym. Sci. Ser. C* 56: 144-153.
- [30] Tiwari, A. 2007. Gum arabic-graft-polyaniline: An electrically active redox biomaterial for sensor applications. *J. Macromol. Sci Part A* 44: 735-745.
- [31] Zhao, X., Lv, L., Pan, B., Zhang, W., Zhang, S., Zhang, Q. 2011. Polymer-supported nanocomposites for environmental application: A review. *Chem. Eng. J.* 170: 381-394.
- [32] Zhu, Y., Murali, S., Cai, W., Li, X., Suk, J.W., Potts, J.R., Ruoff, R.S. 2010. Graphene and graphene oxide: Synthesis, properties, and applications. *Adv. Mater.* 22: 3906-3924.
- [33] Golsheikh, A.M., Lim, H.N., Zakaria, R., Huang, N.M. 2015. Sonochemical synthesis of reduced graphene oxide uniformly decorated with hierarchical znsnanospheres and its enhanced photocatalytic activities. *RSC Adv.* 5: 12726-12735.
- [34] Zhang, K., Zhang, L.L., Zhao, X., Wu, J. 2010. Graphene/polyanilinenanofiber composites as supercapacitor electrodes. *Chem. Mater.*, 22: 1392-1401.
- [35] Huang, X., Qi, X., Boey, F., Zhang, H. 2012. Graphene-based composites. *Chem. Soc. Rev.* 41: 666-686.
- [36] Stoller, M.D., Park, S., Zhu, Y., An, J., Ruoff, R.S. 2008. Graphene-based ultracapacitors. *Nano Lett.* 8: 3498-3502.
- [37] Kuilla, T., Bhadra, S., Yao, D., Kim, N.H., Bose, S., Lee, J.H. 2010. Recent advances in graphene based polymer composites. *Prog. Polym. Sci.* 35: 1350-1375.
- [38] Jahan, M., Bao, Q., Yang, J.X., Loh, K.P. 2010. Structure-directing role of graphene in the synthesis of metal-organic framework nanowire. *J. Am. Chem. Soc.* 132: 14487-14495.
- [39] Petit, C., Bandosz, T.J. 2010. Enhanced adsorption of ammonia on metal-organic framework/graphite oxide composites: Analysis of surface interactions. *Adv. Funct. Mater.* 20: 111-118.
- [40] Jasuja, K., Berry, V. 2009. Implantation and growth of dendritic gold nanostructures on graphene derivatives: Electrical property tailoring and Raman enhancement. *ACS Nano* 3: 2358-2366.
- [41] Wang, H., Hao, Q., Yang, X., Lu, L., Wang, X. 2009. Graphene oxide doped polyaniline for supercapacitors. *Electrochem. Commun.* 11: 1158-1161.
- [42] Kumar, N.A., Choi, H.J., Shin, Y.R., Chang, D.W., Dai, L., Baek, J. B. 2012. Polyaniline-grafted reduced graphene oxide for efficient electrochemical supercapacitors. *ACS Nano* 6: 1715-1723.
- [43] Yong, Y.C., Dong, X.C., Chan-Park, M.B., Song, H., Chen, P. 2012. Macroporous and monolithic anode based on polyaniline hybridized three-dimensional graphene for high-performance microbial fuel cells. *ACS Nano* 6: 2394-2400.
- [44] Shahabuddin, S., Sarih, N.M., Mohamad, S., AtikaBaharin, S.N. 2016. Synthesis and characterization of Co_3O_4 nanocube-doped polyanilinenanocomposites with enhanced methyl orange adsorption from aqueous solution. *RSC Adv.* 6: 43388-43400.
- [45] Zhang, Z., Kong, J. 2011. Novel magnetic Fe_3O_4 @C nanoparticles as adsorbents for removal of organic dyes from aqueous solution. *J. Hazard. Mater.* 193: 325-329.
- [46] Nassar, M.Y., Ahmed, I.S. 2012. Template-free hydrothermal derived cobalt oxide nanopowders: Synthesis, characterization, and removal of organic dyes. *Mater. Res. Bull.* 47: 2638-2645.
- [47] Setshedi K.Z., Bhaumik M., Onyango M.S., Maity A. 2015. *Chem. Eng. J.* 262: 921.
- [48] Wang H., Yuan X., Wu Y., Chen X., Leng L., Wang H., Li H., Zeng G. 2015. *Chem. Eng. J.* 262: 597

- [49] Hummers, W.S., Offeman, R.E. 1958. Preparation of graphitic oxide, *Journal of American Chemical Society* 80: 1339-1339.
- [50] Mahanta, D., Madras, G., Radhakrishnan, S., Patil, S. B 2008, *J. Phys.Chem.* 112: 10151-10157.
- [51] Mahanta, D., Madras, G., Radhakrishnan, S., Patil, S. 2009. Adsorption and Desorption Kinetics of Anionic Dyes on Doped Polyaniline. *Journal of Physical Chemistry B* 113: 2293-2299.
- [52] Nethravati, C., Rajamathi M. 2008. Chemically modified graphene sheets produced by the solvothermal reduction of colloidal dispersions of graphite oxide. *Carbon* 46: 1994-1998.
- [53] Zhu, P., Shen M., Xiao, S., Zhang P., 2011. *Physica B: condensed matter* 406: 498.
- [54] Pham V. H., Coung T. V., Hur S. H., Oh E., Kim K. J., Shin E. W., Chung J. S. 2011. *J. mater chem.* 21: 3371.
- [55] Razak SIA., Ahmad AL., Zein SHS. 2009. *J. Phys. Sci.* 20-27.
- [56] Wu. Z., Chem. X., Zhu, S., Zhou, Z., Yao, Y, Quan, W., Liu, B. 2013. Room temperature methane sensor based on grapheme nanosheets/polyanilinenanocomposite thin film. *IEEE Sens. J.* 13: 777-782.
- [57] Rahy, A., Yang, D.J. 2008. Synthesis of highly conductive polyanilinenanofibers. *Mater. Lett.* 62: 4311-4314.
- [58] Shi, L., Wang, X., Lu, L., Yang, X., Wu, X. 2009. Preparation of TiO₂/polyanilinenanocomposite from a lyotropic liquid crystalline solution. *Synth. Metals.* 159: 2525-2529.
- [59] Ayad, M.M., Abu El-Nasr, A. 2010. Adsorption of Cationic Dye (Methylene Blue) from Water Using Polyaniline Nanotubes Base. *Journal of Physical Chemistry C* 114: 14377-14383.
- [60] Nebi, M.C., Mahjoub, B., Seffen, M. 2007. *J. Hazard. Mater.* B139: 280-285.
- [61] Waranusantigul, P., Poketthitayuk, P., Kuatrachue, M., Upathum, E. S. 2003. 125: 385-392.
- [62] Weng, C.H., Pan, Y.F. 2007. *J. Hazard. Mater.* 144: 355-362.
- [63] Han, R., Wang, Y., Hang, P., Shi, J., Yang, J., Lu, Y. 2006. B137: 550-557.
- [64] Annadurai, G., Juang, R.S., Lee, D.J. 2002. *J. Hazard. Mater.* B92: 263-274.
- [65] Nandi, B., Goswami, A., Purkait, M. 2009. *Applied clay sci.* 42 (3-4): 583-590.
- [66] Crini, G., Peinly, H.N., Gimbert, F., Robert, C. 2007. Separation and Purification Technology 53: 97-110.
- [67] Mahony, T.O., Guibal, E., Tobin, J.M. 2002. 31: 456-463.
- [68] Dogan, M., Alkan, M., Turkyilmaz, A., Ozdemir, Y. 2004. Kinetics and mechanism of removal of methylene blue by adsorption onto perlite. *J. Hazard. Mater.* B109: 141-148.
- [69] Almeida, C.A.P., Debacher, N.A., Downs, A.J., Cottet, L., Mello, C.A.D. 2009. *Journal of Colloid and Interface Science* 332: 46-53.
- [70] Laila Al-Khatib, Feras Fraige, Mohammd Al-Hwaiti, Omar Al-Khashman, 2012. Adsorption from aqueous solution onto natural and acid activated bentonite. *American Journal of Environmental Science* 8(5): 510-522.
- [71] Gurses, A., Dogar, C., Yalcin, M., Acikyildiz, M., Bayrak, R., Karaca, S. 2006. The adsorption kinetics of the cationic dye methylene blue onto clay. *J. Hazard. Mater.* 31: 217-228.
- [72] Banat, F., Al-Asheh, S., Al-Ahmad, R., Bni-Khalid, F. 2007. Bench-scale and packed bed sorption of methylene blue using treated olive pomace and charcoal. *Bioresour. Technol.* 98: 3017-3025.
- [73] BasavaRao, V.V., Mohan Rao, S.R. 2006. Adsorption studies on treatment of textile dyeing industrial effluent by fly ash. *Chem. Eng. J.* 116: 77-84.
- [74] Saniz-Diaz, C., Griffiths, A. 2000. Activated carbon from solid wastes using a pilotscale batch flaming pyrolyser. *Fuel* 79: 1863-1871.
- [75] Tamai, H., Kakii, T., Hirota, Y., Kumamoto, T., Yasuda, H. 1996. Synthesis of extremely large mesoporous activated carbon and its unique adsorption for giant molecules. *Chem. Mater.* 8: 454-462.
- [76] Banat, F., Al-Asheh, S., Al-Makhadmeh, L. 2003. Evaluation of the use of raw and activated date pits as potential adsorbents for dye containing waters. *Process Biochem.* 39: 193-202.

- [77] Kavitha, D., Namasivayam, C. 2007. Experimental and kinetic studies on methylene blue adsorption by coir pith carbon. *Bioresour. Technol.* 98: 14-21.
- [78] Dogan, M., Alkan, M., Onager, Y. 2000. Adsorption of methylene blue from aqueous solution onto perlite, *Water Air Soil Pollut.* 120: 229-248.
- [79] Woolard, C., Strong, J., Erasmus, C. 2002. Evaluation of the use of modified coal ash as a potential sorbent for organic waste streams, *Appl. Geochem.* 17: 1159-1164.
- [80] Ghosh, D., Bhattacharyya, K.G. 2002. Adsorption of methylene blue on kaolinite. *Appl. Clay Sci.* 20: 295-300.
- [81] Chakrabarti, S., Dutta, B.K. 2005. Note on the adsorption and diffusion of methylene blue in glass fibers. *J. Colloid Interface Sci.* 286: 807-811.
- [82] Ncibi, M.C., Hamissa, A.M.B., Fathallah, A., Kortas, M.H., Baklouti, T., Mahjoub, B., Seffen, M. 2009. Biosorptive uptake of methylene blue using Mediterranean green alga *Enteromorpha* spp. *J. Hazard. Mater.* 170: 1050-1055.
- [83] Fu, Y., Viraraghavan, T. 2000. Removal of a dye from an aqueous solution by the fungus *Aspergillus niger*. *Water Qual. Res. J. Can.* 35 (1): 95-111.
- [84] Wang, S., Ma, Q., Zhu, Z.H. 2008. Characteristics of coal fly ash and adsorption application. *Fuel* 87: 3469-3473.
- [85] Janos, P., Buchtova, H., Ryznarova, M. 2003. Sorption of dyes from aqueous solution onto fly ash. *Water Res.* 37: 4938-4944.
- [86] Wang, S., Boyjoo, Y., Choueib, A.A. 2005. Comparative study of dye removal using fly ash treated by different methods. *Chemosphere* 60 () 1401-1407.
- [87] Low, K.S., Lee, C.K. 1990. The removal of cationic dyes using coconut husk as an absorbent. *Pertanika* 13: 221-228.
- [88] Oliveira, L.S., Franca, A.S., Alves, T.M., Rocha, S.D.F. 2008. Evaluation of untreated coffee husks as potential biosorbents for treatment of dye contaminated waters. *J. Hazard. Mater.* 155: 507-512.
- [89] Ferrero, F. 2007. Dye removal by low cost adsorbents: hazelnut shells in comparison with wood sawdust. *J. Hazard. Mater.* 142: 144-152.
- [90] Vadivelan, V., Kumar, K.V. 2005. Equilibrium, kinetics, mechanism, and process design for the sorption of methylene blue onto rice husk. *J. Colloid Interface Sci.* 286: 90-100.
- [91] McKay, G., Ramprasad, G., Pratapamowli, P. 1986. Equilibrium studies for the adsorption of dyestuffs from aqueous solution by low-cost materials. *Water Air Soil Pollut.* 29: 273-283.
- [92] Annadurai, G., Juang, R., Lee, D. 2002. Use of cellulose-based wastes for adsorption of dyes from aqueous solutions. *J. Hazard. Mater.* B92: 263-274.
- [93] Bulut, Y., Aydin, H.A. 2006. Kinetics and thermodynamics study of methylene blue adsorption on wheat shells. *Desalination* 194: 259-267.
- [94] Dogan, M., Alkan, M. 2003. Adsorption kinetics of methyl violet onto perlite. *Chemosphere* 50: 517-528.
- [95] Alkan, M., Dogan, M. 2003. Adsorption kinetics of "yklan" yia blue onto perlite. *Fresenius Environ Bull.* 12(5): 418-425.
- [96] Dogan, M., Alkan, M. 2003. Removal of methyl violet from aqueous solutions by perlite. *J. Colloid Interface Sci.* 267: 32-41.
- [97] Malik, P.K. 2003. Use of activated carbons prepared from sawdust and rice husk for adsorption of acid dyes: a case study of acid yellow36. *Dyes Pigments* 56: 239-249.
- [98] Bouberaka, Z., Khenifi, A., Benderdouche, N., Derriche, Z. 2006. *J. Hazard. Mater.* 133: 154.
- [99] Salleh, MAM., Mohmoud, DK., Karim, WAWA. 2011. *Desalination* 280: 1-13.
- [100] Wu, F., Tseng, R., Juang, R. 2001. *Water Research.* 35: 613.
- [101] Chiou, M.S., Li, H.Y. 2002. *Journal of Hazardous Materials.* 93: 233.
- [102] Ho, Y.S., Chiang, T.H., Hsueh, Y.M. 2005. Removal of basic dye from aqueous solutions using tree fern as a biosorbent. *Process Biochem.* 40: 119-124.
- [103] Dogan, M., Alkan, M., Demirbas, O., Ozdemir, Y., Ozmetin, C. 2006. Adsorption kinetics of maxilon blue GRL onto sepiolite from aqueous solutions. *Chem, Eng. J.* 124: 89-101.
- [104] Pavel, J., Hana, B., Milena, R. 2003. Sorption of dyes from aqueous solutions onto fly ash. *Water Res.* 37: 4938-4944.

- [105]Uzun, 2006. Dyes Pigments. 70: 76.
- [106]Ho YS., Ng JCY., McKay G. 2000. Sep Purif Methods 29-189.
- [107]McKay G., Ho YS. 1999. Process Biochem. 34-45.
- [108]Weber,W.J., Morris, J.C. 1963. Journal of Sanitary Engineering Division ASCE. 89: 31.
- [109]Wu, F., Tseng, R., Juang, R. 2001. Water Research. 35: 613.
- [110]Langmuir, I. 1918. Journal of the American Chemical Society. 40: 1361.
- [111]Langmuir, I. 1916. Journal of the American Chemical Society. 38: 2221.
- [112]Weber, T.W., Chakravorti, R.K. 1974. Journal of American Institute of Chemical Engineering. 20: 228.